Filamentation of focused and collimated laser beams in liquids

D. V. Apeksimov,[1] O. A. Bukin,[2] S. S. Golik,[3] A. A. Zemlyanov,[1] A. M. Kabanov,[4] O. I. Kuchinskaya,[4] G. G. Matvienko,[1] V. K. Oshlakov,[1] A. V. Petrov,[1] E. B. Sokolova,[1] and E. E. Khoroshaeva[1]
[1]V. E. Zuev Institute of Atmospheric Optics SB RAS, Tomsk, Russia; [2]Institute of Automation and Control Processes of the Far Eastern Branch of the Russian Academy of Sciences, Vladivostok, Russia; [3]Far Eastern Federal University, Vladivostok, Russia; [4]National Research Tomsk State University, Tomsk, Russia.

ABSTRACT

Experimental results of investigations into the transformation of the spectral and spatial characteristics of femtosecond collimated and focused Ti:Sapphire-laser beams with wavelengths of 800 and 400 nm upon filamentation in continuous liquid media are presented. It is shown that broadening of the laser pulse spectrum due to phase self-modulation in the medium with a cubic nonlinearity depends on the pulse power and beam diameter. Dependences of the number of filaments, width of laser radiation spectrum, nonlinear focusing distance, and diameter of the filamentation region on the laser pulse power are measured. The existence of a relative power interval in which the explosive growth of the number of filaments occurs, is established.

Keywords: laser radiation, filamentation, femtosecond pulse, liquid, spectrum.

1 INTRODUCTION

In problems of nonlinear femtosecond atmospheric and oceanic optics, the most interesting nonlinear effects, promising for practical application, that accompany the propagation of high-power ultrashort laser pulses is the filamentation of laser beams leading to the transformation of the spectral and spatial characteristics of radiation [1, 2]. In condensed media (liquids and transparent solids), the critical self-focusing power is lower by several orders of magnitude than in gases. That is why the first filamentation of laser beams was obtained in liquids [3]. Despite this, the quantitative filamentation parameters (self-focusing distance, length of the filamentation region, number of filaments in the beam, etc.) in gases have been studied in more detail [2, 4, 5] than in liquids.

2 EXPERIMENTAL RESULTS

This paper presents the results of numerous experimental investigations of the propagation of collimated and focused laser beams in distilled and sea waters and in glycerin. The experiments were performed using test benches developed at Far Eastern Federal University and Institute of Automation and Control Processes of the Far Eastern Branch of the Russian Academy of Sciences in collaboration with Institute of Atmospheric Optics of the Siberian Branch of the Russian Academy of Sciences [6]. In the experiments, radiation of a Ti:Sapphire-laser with a pulse duration of 45 fs at half maximum and gigawatt power at the fundamental (800 nm) and second harmonics (400 nm) was used. The block diagram of the experimental setup is shown in Fig. 1. The emission spectra were registered upon filamentation in cell *11* in integrating sphere *18* in the forward direction and at an angle of 90° to the laser beam axis. Photo- and video recorders *14* and *15* were used to record the filamentation. The laser beam with a diameter of 7 or 9 mm was focused as needed by the lens with a focal length of 50/2 mm into the cell center. The laser pulse power was varied by changing the laser pump power and pulse duration with compressor *2* and was monitored using power and energy meter *7* and autocorrelator *5*. The beam quality was controlled with beam profiler *9*. Upon filamentation of the pulse with the wavelength $\lambda = 800$ nm in distilled water (Fig. 2), the broadening of the spectrum (Fig. 2*a*) was observed caused by the phase self-modulation in the medium with a cubic Kerr nonlinearity and the displacement of its center of mass toward shorter wavelengths due to plasma nonlinearity. These effects were the stronger, the higher was the initial pulse power (curve *1* in Fig. 2*a*). Thus, for pulse energy of 1 mJ (curve *2* in Fig. 2) which corresponded to ~15 GW power, that is, for the parameter $\eta = P/P_{cr} \sim 2.5 \cdot 10^3$ (the nonlinear correction of the refractive index for water upon exposure to

21st International Symposium on Atmospheric and Ocean Optics: Atmospheric Physics, edited by G. G. Matvienko, O. A. Romanovskii, Proc. of SPIE Vol. 9680, 96801X
© 2015 SPIE · CCC code: 0277-786X/15/$18 · doi: 10.1117/12.2205790

radiation with $\lambda = 800$ nm is $n_2 = 2.0 \cdot 10^{-16}$ cm^2/W and the critical self-focusing power is $P_{cr} = 6.5$ MW [7, 8]), the spectrum encompassed practically the entire visible range and a part of the near-IR range. For a comparison, curve *4* in Fig. 2*a* shows the spectrum of the laser pulse of the same power upon filamentation in air [9]. As follows from a comparison of spectra *2* and *4*, the spectrum width at e^{-2} level upon filamentation in water is 5 times greater than in air. The spectrum width decreased by a factor of 3.5 when the parameter η decreased 20 times, that is, for $\eta \sim 123$ (curve *3* in Fig. 2*a*), but exceeded the width of the initial spectrum by a factor of 1.5.

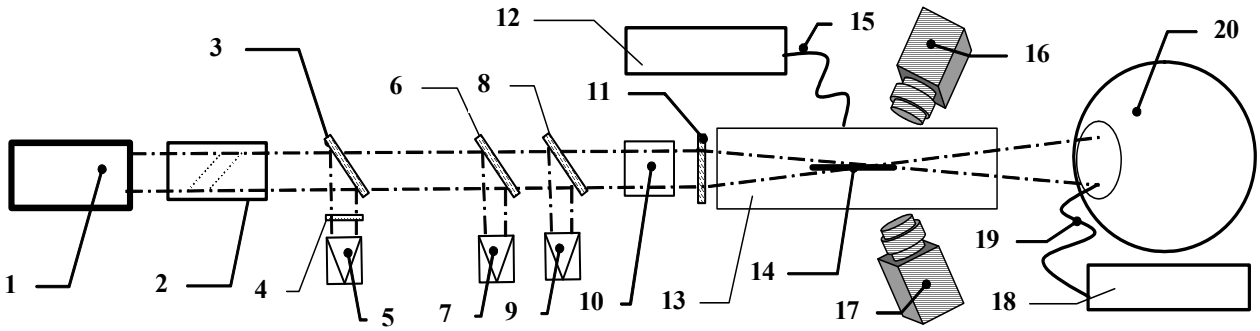

Fig. 1. Block diagram of the experimental setup comprising laser system *1* with $\lambda_{01} = 800$ nm, $E_{01} = 1$ mJ, $\lambda_{02} = 400$ nm, $E_{02} = 0.3$ mJ, pulse repetition frequency of 1 kHz, $t_p = 35$ fs, and $d = 7$ mm (Spitfire Pro 40F, Spectra Physics); compressor 2; rotating plates *3*, *6*, and *8*; filter *4*; PSCOUT PL-SP-LF autocorrelator (Spectra Physics) *5*; 407A energy meter (Spectra Physics) *7*; beam profiler *9*; beta barium borate BBO (β-BaB_2O_4) conversion crystal *10* at 300 μm; removable focusing lens (BK7 plano-convex lens with $d \sim 6$ mm) *11* with $f = 50.2$ mm; Maya 2000Pro spectrometer *12*; cell *13* with length $L = 10$ cm and thickness of the input window of 150 μm that was filled with water; filamentation region *14*; optical waveguides *15* and *19*; JVC GZ-MG255 video camera *16*; SONY DSC-F828 camera *17*; HR4000 spectrometer (Ocean Optics) *18*; and integrating sphere *20*.

As can be seen from the photograph (Fig. 2*b*), the filament is formed at the beginning of the cell for $\eta \sim 2.5 \cdot 10^3$, which is confirmed by the divergent luminescent beam in the visible region of the spectrum corresponding to generation of the supercontinuous luminescence upon filamentation of the beam registered by the camera. By the middle of the cell, near the geometrical focus of the lens, this luminescent beam converges, and luminous plasma formations are observed in the region of the beam waist; therefore, an intensity of $\sim 10^{11}$ W/cm^2 is attained there.

For the second harmonic at 400 nm ($n_2 \sim 5 \cdot 10^{-16}$ cm^2/W [7, 8]), the filamentation region in water is also broadened (Fig. 3*a*) in comparison with the initial pulse, but its shift toward longer wavelengths is observed. The same Stokes shift was observed by the authors in [9] upon filamentation excited by the second harmonic in air.

Figure 3*a* shows the Raman scattering (RS) spectra in sea and distilled waters excited by the second harmonic of the femtosecond Ti:Sapphire laser. The spectral band describing the initial pulse of incident radiation at 25000 cm^{-1} (Rayleigh scattering at 400 nm) was the etalon band. Against its background, the difference between the RS bands in distilled and sea waters caused by internal and intermolecular interactions is clearly pronounced. The characteristic shifts of the emission bands toward longer wavelengths were observed in both cases, which demonstrated the presence of Stokes scattering. The maximum value of the band intensities in sea and distilled waters were observed at 21551 cm^{-1}, that is, the frequency shift of the Raman scattering was equal to 3449 cm^{-1}.

The band intensity in distilled water had a clear-cut profile in contrast with the band in sea water samples. In the case of the latter, an increase in the band width toward longer wavelengths and a slow decrease of the band intensity were clearly pronounced. This circumstance is due to the presence of biogenic suspensions (fragments of bodies and excrements of pelagic organisms) and dissolved organic matter (DOM). Among the biogenic suspensions are fluorescent natural compounds such as proteins and aromatic amino acids, nucleic acids, phenols and polyphenolic compounds (lignin and tannin), humic compounds and their components, as well as some pigments. In [10, 11], luminescence in the visible range of the spectrum with maximum at 400–450 nm was explained by the presence of fluorescing humic compounds in sea water. In this case, Fig. 3*a* demonstrates that upon excitation by femtosecond pulses at a wavelength of 400 nm, the spectral band has equivalent broadening caused also by the overlap of broad bands of the vibrational system of the hydroxyl group in the water molecule and fluorescence of the humic compounds.

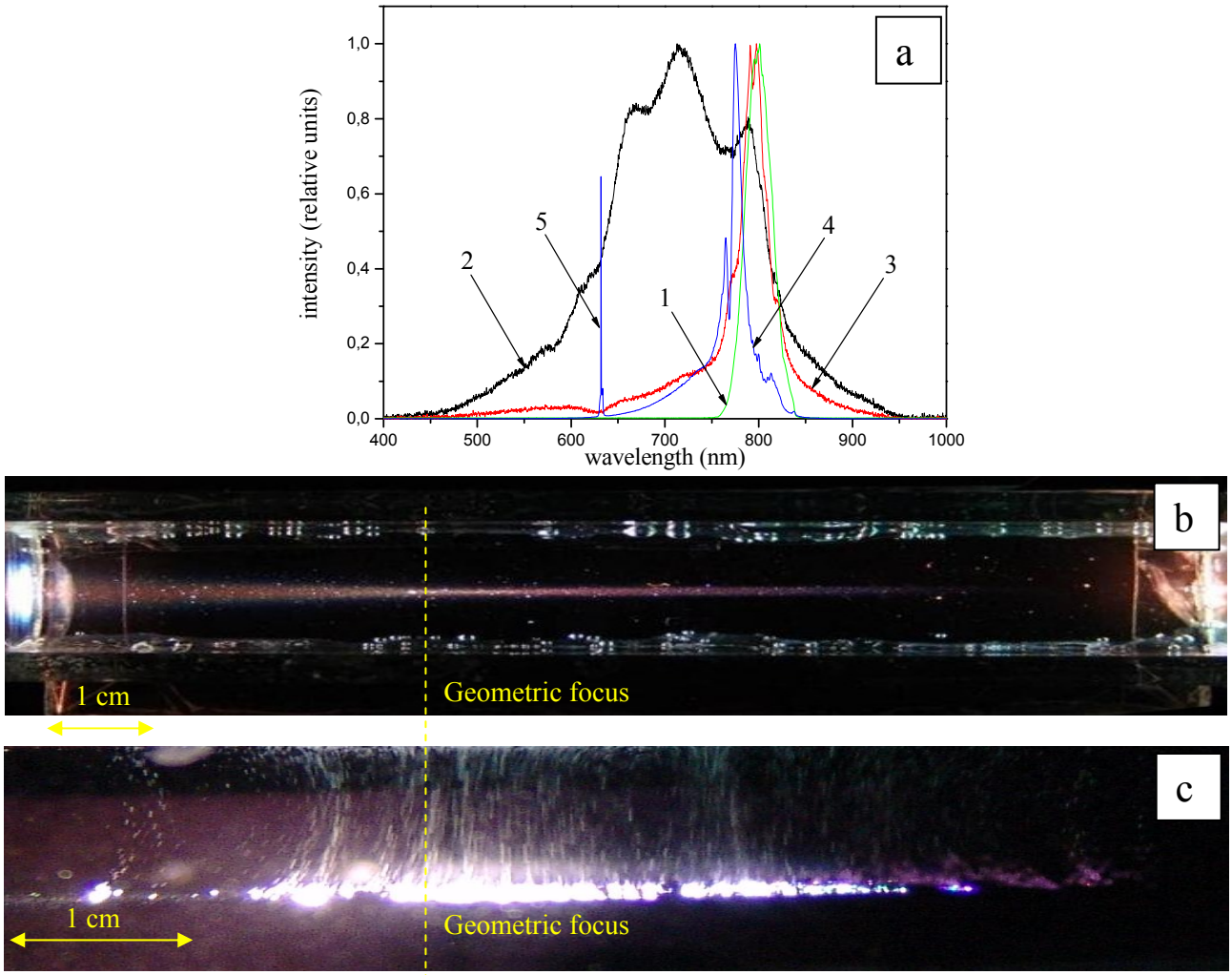

Fig. 2. Spectra of the fundamental harmonic of a femtosecond laser pulse ($\lambda = 800$ nm) upon filamentation. Here curve *1* is for the spectrum of the initial pulse (reflection from the scattering ceramic surface), curve *2* is for the filamentation pulse with $t_p = 35$ fs and $E = 1$ mJ in distilled water, curve *3* is for $t_p = 700$ fs and $E = 1$ mJ in distilled water, curve *4* is for $t_p = 35$ fs and $E = 1$ mJ in air (curves *2*, *3*, and *4* were measured in the integrating sphere in the forward direction with the HR4000 spectrometer), and curve *5* is for the continuous He–Ne-laser spectrum (for a comparison). Hereinafter, normalization by the maximum intensity (*a*) is used. Photographs upon filamentation of pulses with $t_p = 35$ fs and $E = 1$ mJ (top view *b*), and $t_p = 700$ fs and E = 1 mJ (side view *c*).

Examples of images of cross sectional areas of collimated laser beams after their filamentation in the cell recorded from the screen are shown in Fig. 4. Bright spots in the images characterize increased energy densities in the beam compared to the average energy level and represent luminous filaments formed on the propagation path. The intensity of the luminous structure is retained along a certain part of the propagation path called the filament length. The transverse sizes of the filamentation region are characterized by the filament radius having a quasi-constant value (5–10 μm for water) and by the number of filaments. In the images it can be seen that the number of *hot spots* formed in the laser beam increases with the initial laser pulse power. The diameter of the region occupied with bright spots, each of which corresponds to a filament in the cell, also increases. Fig. 4*e* shows the image of the laser beam structure recorded from the screen upon filamentation in water with hydrosols (0.5 ml of bifidumbacterin (curved rods 2–5 mm long) per 40 ml of water) 30 s after the beginning of irradiation. The image shows that the addition of hydrosols to distilled water leads to a redistribution of the cross sectional structure of the filamentation region. This is most likely caused by the formation of convective flows in the cell.

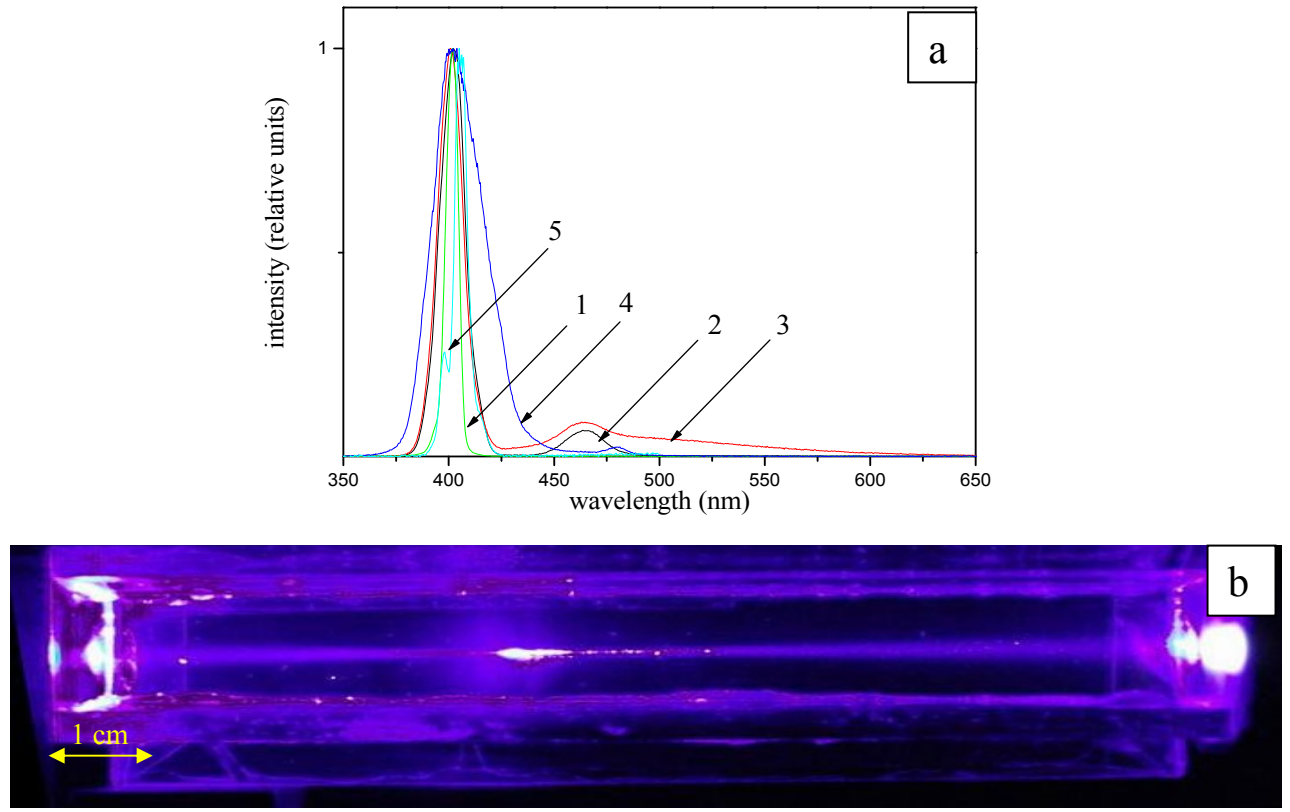

Fig. 3. Spectra of the second harmonic of a femtosecond laser pulse ($\lambda = 400$ nm) upon filamentation. Here curve *1* is for the spectrum of the initial pulse (reflection from the scattering ceramic surface), curve *2* is for the filamentation of the pulse with $E = 0.3$ mJ in distilled water, curve *3* is for the filamentation of the pulse with $E = 0.3$ mJ in seawater (curves *2* and *3* were measured in the filamentation region with the Maya spectrometer tilted at an angle of 90° to the beam), curve *4* is for the filamentation of the pulse with $E = 0.3$ mJ in distilled water, and curve *5* is for the filamentation of the pulse with $E = 0.3$ mJ in air (curves *4* and *5* were measured with the spectrometer HR4000 in the integrating sphere in the forward direction) (*a*). Photographs of filamentation of the pulse with $E = 0.4$ mW in water (top view *b*).

Fig. 5 shows the dependence of the number of hot spots on the ratio of the initial laser pulse power to the critical self-focusing power ($P_{cr} = 6.5$ MW for water [7]). The existence of the interval of relative power values ($P/P_{cr} > 3000$) is clearly pronounced in which a sharp increase of the number of hot spots is observed. This is due to the corresponding increase of the number of filaments. When the power increment reached about 10 times, the number of the above-indicated points increased approximately 300 times.

Figure 6 shows photographs of the filamentation in the cell for the indicated values of the initial laser pulse power. As can be seen from the photographs, an increase in the average pulse power leads first, to the increase of the diameter of the filamentation region, and second, the beginning of this filamentation region is shifted toward the source.

The dependences of the diameter of the filamentation region and of the distance of filamentation beginning on the laser pulse power are shown in Figs. 7 and 8, respectively. Figure 8, in addition to the experimental data (squares), shows the dependence of the distance of filamentation beginning calculated from the Marburger formula (circuits). Satisfactory agreement between the calculated and experimental data can be obtained if we decrease 7 times the calculated values.

The transformation of the radiation spectrum upon filamentation in water was measured using the integrating sphere located behind the cell and the Maya 2000 Pro spectrometer (Ocean Optics) by the two methods in which the power was varied by changing the energy or the pulse duration depending on the pulse power. The plot in Fig. 9 shows that broadening of the spectra obtained by the first and second methods are comparable in values and the spectra encompass the entire range of the visible spectrum.

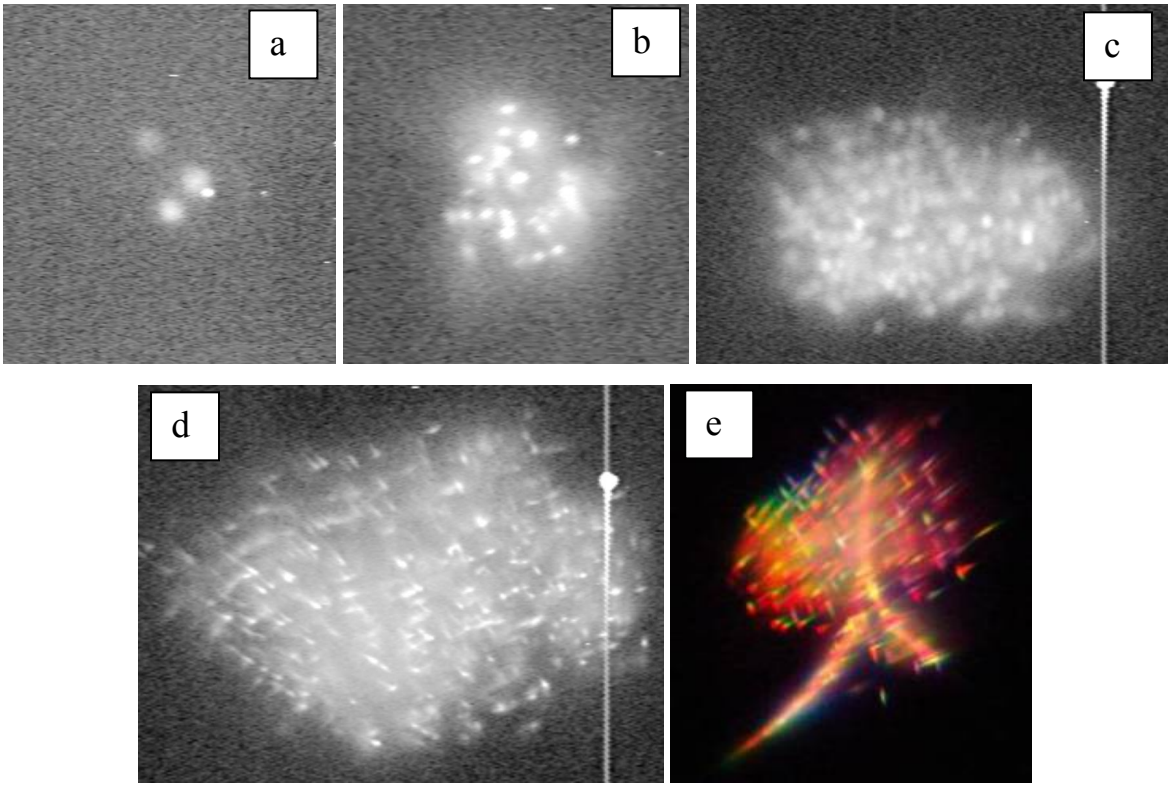

Fig. 4. Images of the structure of the laser beam after its filamentation in the cell filled with water registered from the screen for laser pulse energies of 1.7 (case *a*), 2.4 (case *b*), 4 (case *c*), and 5.2 mJ (case *d*); case *e* is for water containing hydrosols 30 s after the beginning of irradiation by periodic laser pulses.

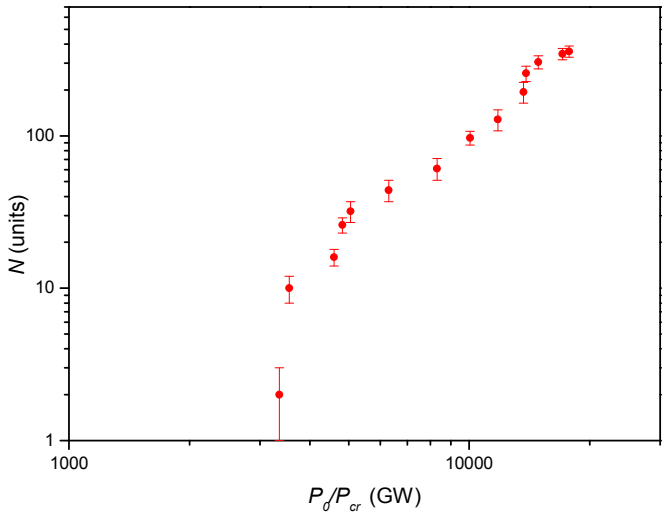

Fig. 5. The dependence of the number N of hot spots registered from the screen on the ratio of the average power P_0 of the laser pulse to the critical self-focusing power P_{cr}.

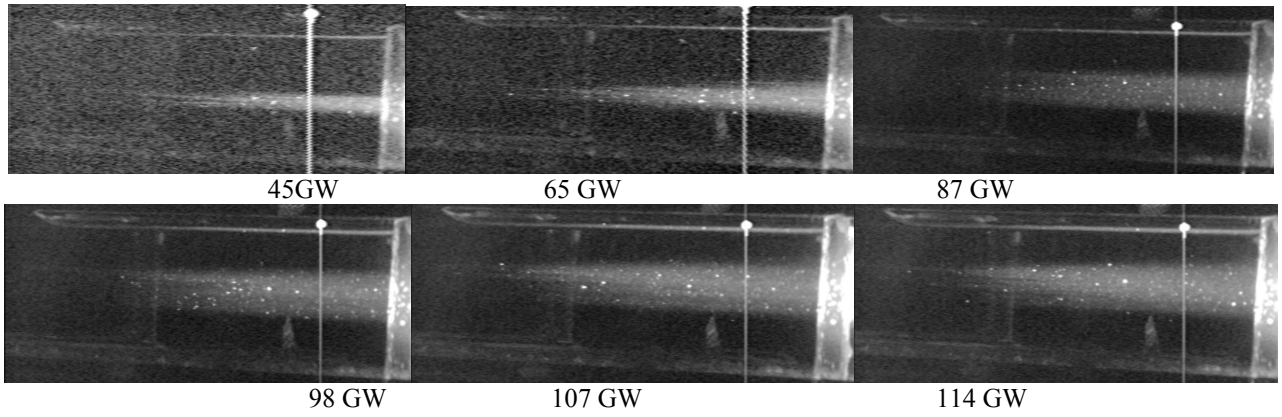

Fig. 6. Images of the filamentation region in the cell for the indicated values of the laser pulse energy.

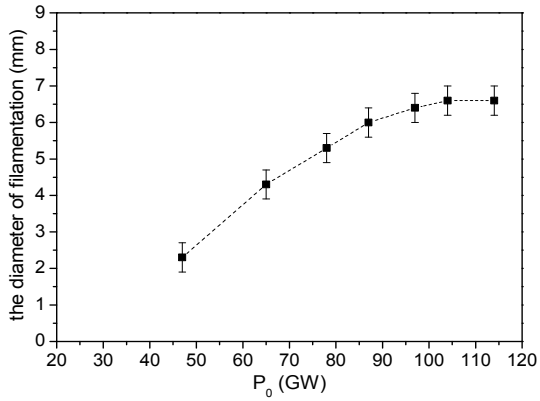

Fig. 7. Dependence of the filamentation region diameter on the average laser pulse power.

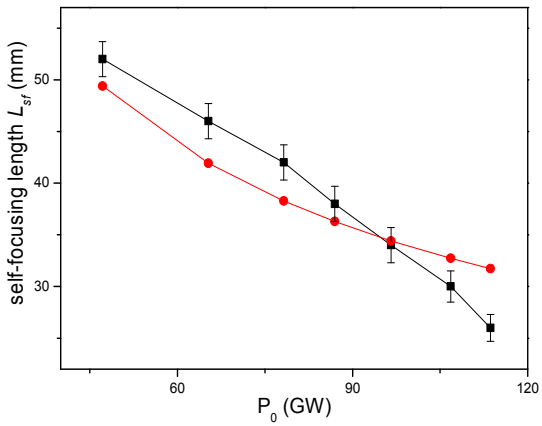

Fig. 8. Dependences of the distance of filamentation beginning on the laser pulse power. Here circles are calculated from the Marburger formula for $2 \cdot 10^{-2} P_{cr}$ and squares are for the experimental data.

This fact allows pulses with equal energies to be generated and used, for example, for a gas analysis in laser optoacoustic spectroscopy in which the magnitude of the acoustic response is proportional to the absorbed light energy when the emission line falls within the absorption line of the examined substance. Currently, laser sources with tunable wavelengths are used for this purpose; however, the range of their tuning is small [12].

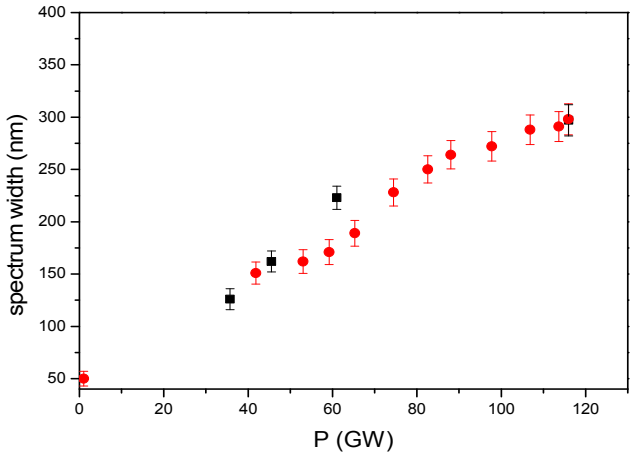

Fig. 9. Dependence of the width of the laser pulse spectrum after filamentation in water on the pulse energy. Here circles illustrate changes in the pulse power attendant to changes of the pulse energy, and squares show the change in the power attendant to changes of the pulse duration.

Thus, experiments on the filamentation of laser beams in liquids have demonstrated that the filamentation upon exposure to the first and second harmonics broadens the spectrum of the initial pulse due to the phase self-modulation. Moreover, the shift of the center of mass and of the spectral maximum toward shorter wavelengths caused by plasma nonlinearity (*blue shift*) is observed upon exposure to the first harmonic, and the shift toward longer wavelengths (*red shift*) is observed upon exposure to the second harmonic. The spectrum of laser pulses having the same power is broadened in water stronger than in air. Upon filamentation in water, the luminescence with the maximum in the region of 464 nm is caused by Raman scattering on stretching vibrations of water molecules. In sea water, the broadening of the luminescence spectrum toward longer wavelengths is due to the superposition of Raman scattering and the fluorescence of organic substances dissolved in water. With increasing initial power of the collimated laser beams, the number of filaments formed in the laser beam increases. In this case, the number of filaments sharply increases when the pulse power reaches ~20 GW. The spectrum of the initial laser pulse upon filamentation in water is broadened the stronger, the higher is the power of the pulse It encompasses the entire visible range for both focused and collimated beams. The magnitude of the spectrum broadening is practically independent of the method of power change by changing the laser pulse length or energy. With increasing laser power, the distance of filamentation beginning decreases and the diameter of the filamentation region increase. This work was supported in part by the Tomsk State University "Academician D.I. Mendeleev Fund Program."

REFERENCES

[1] Y. R. Shen, R. W. Boyd, and S. G. Lukishova, eds., Self-focusing: Past and Present, Springer, New York (2009).
[2] Yu. E. Geints, A. A. Zemlyanov, A. M. Kabanov, and G. G. Matvienko, Nonlinear Femtosecond Atmospheric Optics, A. A. Zemlyanov, ed. [in Russian], Publishing House of the Institute of Atmospheric Optics of the Siberian Branch of the Russian Academy of Sciences, Tomsk (2010).
[3] N. F. Pilipetskii and A. R. Rustamov, JETP Lett., **2,** 55 (1965).
[4] S. L. Chin, Femtosecond Laser Filamentation, Springer Series on Atomic, Optical, and Plasma Physics, **55**, DOI: 10.1007/978-1-4419-0688-5.
[5] D. V. Apeksimov, O. A. Bukin, E. E. Bykova, *et al*., Atm. Oceanic Opt., **26**, No. 3, 171–177 (2013).
[6] O. A. Bukin, E. E. Bykova, Yu. E. Geints, *et al*., Atm. Oceanic Opt., **24**, No. 5, 417–424 (2011).
[7] Yu. E. Geints and A. A. Zemlyanov, Opt. Atmosf. Okeana, **22**, No. 9, 749–756 (2010).
[8] Yu. E. Geints and A. A. Zemlyanov, Opt. Atmosf. Okeana, **22**, No. 9, 757–760 (2010).
[9] Yu. E. Geints, A. M. Kabanov, A. A. Zemlyanov, *et al*., Appl. Phys. Lett., **99**, 181114-1-3 (2011), DOI: 10.1063/1.3657774.
[10] O. A. Bukin, S. S. Golik, P. A. Salyuk, *et al*., J. Appl. Spectrosc., **74**, No. 1, 115–119 (2007).
[11] O. M. Gorshkova, S. V. Patsaeva, E. V. Fedoseeva, *et al*., Water: Chem. Ecol., **11**, 31–37 (2009).
[12]B. G. Ageev, Yu. V. Kistenev, E. P. Krasnozhenov, *et al*., Opt. Atmosf. Okeana, **21**, No. 12, 1108–1114 (2008).